

This article was downloaded by:

On: 26 January 2011

Access details: *Access Details: Free Access*

Publisher *Taylor & Francis*

Informa Ltd Registered in England and Wales Registered Number: 1072954 Registered office: Mortimer House, 37-41 Mortimer Street, London W1T 3JH, UK



Liquid Crystals

Publication details, including instructions for authors and subscription information:

<http://www.informaworld.com/smpp/title~content=t713926090>

Electric field effects in nematic layers with weak boundary anchoring

G. Derfel^a

^a Institute of Physics, Technical University of Łódź, Łódź, Poland

To cite this Article Derfel, G.(1991) 'Electric field effects in nematic layers with weak boundary anchoring', *Liquid Crystals*, 10: 1, 29 – 34

To link to this Article: DOI: 10.1080/02678299108028226

URL: <http://dx.doi.org/10.1080/02678299108028226>

PLEASE SCROLL DOWN FOR ARTICLE

Full terms and conditions of use: <http://www.informaworld.com/terms-and-conditions-of-access.pdf>

This article may be used for research, teaching and private study purposes. Any substantial or systematic reproduction, re-distribution, re-selling, loan or sub-licensing, systematic supply or distribution in any form to anyone is expressly forbidden.

The publisher does not give any warranty express or implied or make any representation that the contents will be complete or accurate or up to date. The accuracy of any instructions, formulae and drug doses should be independently verified with primary sources. The publisher shall not be liable for any loss, actions, claims, proceedings, demand or costs or damages whatsoever or howsoever caused arising directly or indirectly in connection with or arising out of the use of this material.

Electric field effects in nematic layers with weak boundary anchoring

by G. DERFEL

Institute of Physics, Technical University of Łódź,
ul. Wólczańska 221, 93-005 Łódź, Poland

(Received 8 January 1991; accepted 1 February 1991)

The stationary states induced by an electric field in nematic layers with weak boundary anchoring are described by means of the Taylor expansion method based on catastrophe theory. The planar, twisted and supertwisted structures are considered. The analysis is extended to materials with negative dielectric anisotropy. Several types of behaviour are found. The possibility of switching between twisted and homeotropic states is suggested.

1. Introduction

The strength of the interaction between the liquid crystal and the substrate determines the boundary conditions governing the equilibrium states of the layer. Its role for the transitions induced by an external field was shown for the first time in [1], where the threshold field was related to the anchoring energy. The effect of finite anchoring forces was investigated theoretically for the planar, homeotropic and twisted nematic layers [2-5]. The problem of finite boundary coupling is important for surface stabilized ferroelectric liquid crystal layers [6]. In [7], the general criteria for the existence of first order transitions in weakly anchored nematic layers were discussed. The role of the finite surface anchoring for the measurement of elastic constants was stressed in [8]. Usually the variational method was used in the calculations. Recently, the influence of the anchoring energy on the critical field for the transition of a planar layer was considered by use of trial functions [9]. The stationary states, which are related with such systems, can be studied by means of the method derived from catastrophe theory [10], as shown for instance in [11] and [12].

In this paper, three kinds of nematic layers are considered with the assumption of weak anchoring: planar, twisted nematic and supertwisted nematic. The role of finite surface anchoring and of some other material and geometrical parameters is investigated. The results are of a qualitative character. Some new effects occurring for materials with negative dielectric anisotropy, $\Delta\epsilon$, are predicted. Other results agree with previous work. The method used here was described in previous papers [11, 12]. It is, therefore, only briefly sketched in §2, where the present problem is formulated. Section 3 contains the results of calculations and section 4 is devoted to discussion.

2. Method

The idea of the method applied here is as follows. The free energy of the layer, G , is expressed as a function of the angles, which are sufficient for the quantitative determination of the director distribution. The critical points of G are found and their degeneracy is investigated. In the vicinity of each degenerate critical point, the function G is reduced to the catastrophe, i.e., to the topologically equivalent function of a standard form. The catastrophe yields a qualitative picture of the behaviour of the layer

at small deformations, since it gives the number and disposition of the equilibrium states of the system in the vicinity of its critical points. The first step of the procedure used for the determination of a suitable catastrophe is an expansion in a Taylor series in the neighbourhood of the chosen critical point. Next the second derivative matrix \mathbf{H} is diagonalized and the non-essential variables are eliminated. This leads to a rather complicated form of the final expansion coefficients. It is useless to write them explicitly and the calculations must be performed numerically. The resulting power series is then limited to the order necessary for a proper description of the system. This order is determined separately. In the situations presented the sixth order terms should be retained; these give rise to the butterfly catastrophe.

It is assumed that the nematic material, characterized by the elastic constants k_{11} , k_{22} , and k_{33} , and dielectric permittivities ε_{\parallel} and ε_{\perp} , is confined between two electrodes, placed parallel to the (xy) plane at $z = \pm d/2$. An intrinsic pitch, 2λ , caused by chiral additives, may be introduced. The directions of the alignment at the lower and upper surfaces are twisted by an angle Φ . It is assumed that they are fixed and do not change under the action of the field. Therefore, the energy of the anchoring at each surface depends only on the surface tilt angle ψ . Its value per unit area is measured by the coefficient γ and may be approximated by

$$g_{\text{surface}} = -\gamma \cos^2 \psi. \quad (1)$$

The director orientation within the layer is determined by the angles θ and ω , between the director and the xy and yz planes, respectively. The electric field is applied along the z axis. The total free energy per unit area of the layer is given by

$$\begin{aligned} G = & \frac{k_{11}}{2} \int_{-d/2}^{d/2} [(\cos^2 \theta + k_b \sin^2 \theta)(\partial\theta/\partial z)^2 + 2k_t(d/\lambda) \cos^2 \theta(\partial\omega/\partial z) \\ & + \cos^2 \theta(k_t \cos^2 \theta + k_b \sin^2 \theta)(\partial\omega/\partial z)^2] dz \\ & - U^2 \Delta\varepsilon\varepsilon_0 \left(2\beta \int_{-d/2}^{d/2} \frac{dz}{1 + \beta \sin^2 \theta} \right)^{-1} - 2\gamma \cos^2 \psi, \end{aligned} \quad (2)$$

where $\beta = \Delta\varepsilon/\varepsilon_{\perp}$, $k_b = k_{33}/k_{11}$, $k_t = k_{22}/k_{11}$ and U is the applied voltage. If small deformations are assumed, then the angles $\theta(z)$ and $\omega(z)$ can be approximated by

$$\theta(z) = \psi + \xi \cos(\pi z/d), \quad (3)$$

$$\omega(z) = \Phi z/d + \chi \sin(2\pi z/d). \quad (4)$$

The energy $G(\xi\psi\chi)$ can be analysed in the vicinity of its critical points.

There are two critical points. The first is due to the undeformed state $\xi = 0$, $\psi = 0$, $\chi = 0$. The second is determined by $\xi = 0$, $\psi = \pi/2$, $\chi = 0$, and is due to the uniform director distribution normal to the plates. In the following, these states will be denoted as the lower and the upper. Both of the critical points are degenerate, i.e., the determinant of the matrix \mathbf{H} vanishes for some sets of parameters. The most significant critical parameter is the threshold value of the applied electric field or voltage.

3. Results

The butterfly catastrophe is obtained from the analysis of the Taylor expansion of G ; it predicts several types of behaviour of the layer. The deformations found in the vicinity of the threshold voltage in the lower and upper states are combined together in

a way similar to that used in [12]. The resulting types of behaviour are presented in figures (a)–(k). The angle $\theta_m = \xi + \psi$, measuring the midplane director orientation, is plotted against the reduced voltage $u = (U/U_c)^2 \Delta\epsilon/|\Delta\epsilon|$. In this way, the left hand part of each diagram illustrates the behaviour for $\Delta\epsilon < 0$ and the right hand part that for $\Delta\epsilon > 0$. Since the method based on catastrophe theory gives qualitative results, only the shapes of the $\theta_m(u)$ dependences are drawn in the figure. The values of the reduced threshold voltage can be very well approximated by means of equation (5) (see later), (the inaccuracy is due to the model character of the functions $\theta(z)$ and $\omega(z)$, defined by equations (3) and (4)). The example sets of parameters, leading to each of the possible situations, are given in the table.

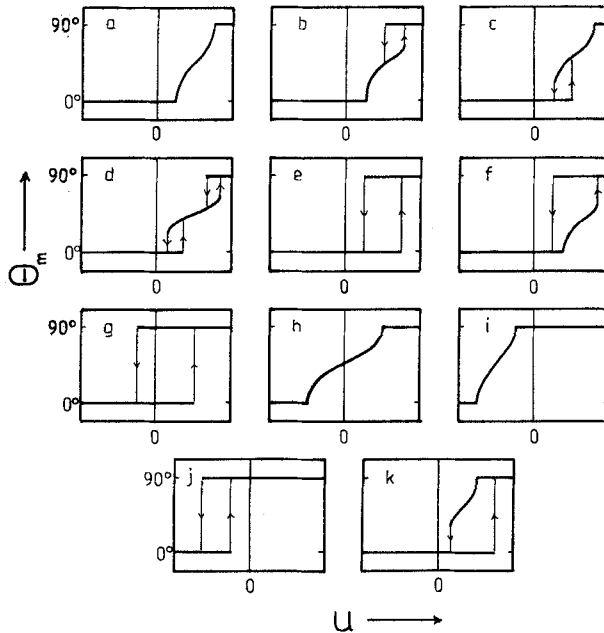
3.1. Thresholds

The threshold voltages for the lower and upper states, denoted as u_1 and u_2 , respectively, are determined by the degeneracy condition $\det \mathbf{H} = 0$. Its solutions have the form

$$u_{1,2} = \frac{-B \pm \sqrt{B^2 - 4AC}}{2A}, \tag{5}$$

where $A = \pi^2 - 8$. For the lower state

$$\left. \begin{aligned} B &= -2(\pi^2 - 8)[(\Phi/\pi)^2(k_b - 2k_i) - 2k_i(d/\lambda)(\Phi/\pi)] - 4\gamma d/k_{11} - \pi^2, \\ C &= (\pi^2 - 8)[(\Phi/\pi)^2(k_b - 2k_i) - 2k_i(d/\lambda)(\Phi/\pi)]^2 \\ &\quad + (\pi^2 + 4\gamma d/k_{11})[(\Phi/\pi)^2(k_b - 2k_i) - 2k_i(d/\lambda)(\Phi/\pi)] + 4\gamma d/k_{11} \end{aligned} \right\} \tag{6}$$



The schematic presentations, (a)–(k), of the shapes of the $\theta_m(u)$ dependence showing the stability of the lower and upper states and the possibilities of transitions between them. The sets of parameters, leading to each situation, are given in the table.

The examples of the parameters leading to various types of behaviour of the nematic cells ($\varepsilon_{\perp} = 7$, $g = \gamma d/k_{11}$).

Figure	Planar				Twisted nematic cell				Supertwisted nematic cell ($\Phi = \pi$, $d = -\lambda$)			
	k_b	k_t	$\Delta\varepsilon$	g	k_b	k_t	$\Delta\varepsilon$	g	k_b	k_t	$\Delta\varepsilon$	g
(a)	1.8	0.7	5.0	5.0	1.8	0.7	2.0	3.0	1.2	0.7	5.0	5.0
(b)	1.8	0.7	9.0	5.0	1.8	0.7	5.0	2.0	1.8	0.7	10.0	5.0
(c)					1.8	0.7	1.0	2.0	1.5	0.7	5.0	5.0
(d)					1.8	0.7	1.5	2.0	1.8	0.7	5.0	5.0
(e)					1.8	0.7	1.0	1.5	1.8	0.7	5.0	3.0
(f)					1.8	0.7	5.0	1.5	1.8	0.7	10.0	3.0
(g)					1.8	0.7	5, -1	0.7	1.8	0.7	5, -1	0.7
(h)					1.0	1.0	5, -1	0.7				
(i)					1.0	1.0	5, -1	0.5				
(j)					1.2	1.0	5, -1	0.5				
(k)									1.5	0.4	1.0	3.0

and for the upper state

$$\left. \begin{aligned} B &= 2(\pi^2 - 8)[(\Phi/\pi)^2 k_b + 2k_t(d/\lambda)(\Phi/\pi)] - 4\gamma d/k_{11} + \pi^2 k_b, \\ C &= (\pi^2 - 8)[(\Phi/\pi)^2 k_b + 2k_t(d/\lambda)(\Phi/\pi)]^2 \\ &\quad + (\pi^2 k_b - 4\gamma d/k_{11})[(\Phi/\pi)^2 k_b + 2k_t(d/\lambda)(\Phi/\pi)] - 4k_b \gamma d/k_{11}. \end{aligned} \right\} \quad (7)$$

From the two possible solutions with equal signs, that with the smaller absolute value is taken for the threshold. The sign of the threshold indicates the sign of the dielectric anisotropy, for which the critical phenomena occur.

Several situations, resulting from the signs of u_1 and u_2 and from the relations between them, are possible: (i) $u_2 > u_1 > 0$, (ii) $u_2 > 0$ and $u_1 < 0$, (iii) $u_1 < u_2 < 0$, (iv) $u_1 > u_2 > 0$, (v) $u_1 > 0$ and $u_2 < 0$, (vi) $u_2 < u_1 < 0$. The details of the deformations in the layer in these situations will be described further. Here, let us note that the cases (i)–(v), include the behaviour of the planar and twisted nematic cells studied in [2] and [5]. The results obtained there agree very well with the values of the corresponding threshold voltages calculated from equation (5), as well as with their dependence on γ . The values of u_1 are also in agreement with results presented in [4].

Four ranges of surface interaction strength can be distinguished. They are denoted as strong, medium, weak and very weak. They correspond to various classes of the behaviour of the layer. Their limits are difficult to specify generally, as they depend on other parameters.

3.2. Planar cell ($\Phi = 0$, $d/\lambda = 0$)

The threshold voltages in this case are always positive: $u_2 > u_1 > 0$. This reflects the obvious fact that the material with $\Delta\varepsilon < 0$ is absolutely stable in the electric field. The behaviour of nematics with a positive dielectric anisotropy is shown in figures (a) and (b). If $\Delta\varepsilon$ is sufficiently high, then the transition from the upper state is discontinuous and a hysteresis is possible. The threshold values tend to zero with decreasing anchoring energy.

3.3. Twisted nematic cell ($\Phi = \pi/2$, $d/\lambda = 0$)

Several types of behaviour are predicted in this system. The relation between u_1 and u_2 is influenced by the anchoring energy coefficient γ and by the relative magnitudes of k_b and k_t . As we can see from equations (6) and (7), the lower threshold depends on the value of the expression $k_b - 2k_t$, whereas the upper threshold depends only on k_b .

For high γ case (i) takes place. The discontinuities may occur at the lower or at the upper transition, or at both. The deformations are illustrated in figures (a)–(d). If the anchoring is of medium strength, then case (iv) occurs. The transitions between the lower and the upper states are discontinuous (see figure (e)). However for high $\Delta\varepsilon$ the deformation of the lower state begins continuously (see figure (f)).

For weak anchoring two possibilities can be distinguished. If k_b differs significantly from k_t , then case (v) takes place and both states can be stable in the absence of the field. Transitions between them are possible given a suitable sign of $\Delta\varepsilon$ and are illustrated in figure (g). The upper state is absolutely stable for positive anisotropy whereas the lower state is stable for the negative case. If $k_b \approx k_t$ then case (ii) occurs. The twisted structure is deformed in the absence of the field. For $\Delta\varepsilon > 0$ the field induces a transition to the upper state, whereas for $\Delta\varepsilon < 0$ the lower state is reached (see figure (h)).

At very weak anchoring, the homeotropic state is stable without the field. Cases (iii) and (vi) are possible depending on the relation between k_b and k_t . The transition to the lower state is possible if $\Delta\varepsilon < 0$ (see figures (i) and (j), respectively).

3.4. Supertwisted nematic cell ($\Phi > \pi/2$, $d/\lambda \neq 0$)

All relations between the upper and the lower thresholds with the exception of (vi) were found in this case. All types of behaviour shown in figures (a)–(g) can take place (the situation presented in figure (h) was not found for typical elastic constants). There exists also another possibility due to case (iv) shown in figure (k).

4. Discussion

The Taylor expansion of the total free energy G contains only even terms. This corresponds to the incomplete form of the butterfly catastrophe. However, because of the complexity of the resulting expressions, no additional perturbation leading to the odd terms, (for example, in the form of the initial surface tilt), was introduced. In some cases discontinuous transitions occur far from the threshold. It is impossible to determine the value of u for such a transition. Therefore, the width of the hysteresis shown in figures (b), (c), (d), (f) and (k) cannot be calculated. The problem of the occurrence of some other similar situations which are potentially possible cannot be solved.

The results obtained here agree with those obtained by others. Some of the possibilities of discontinuous transitions discussed in [7] are found for the twisted structures. However the behaviour of the twisted nematic layer at the upper state predicted in [4] does not correspond to any catastrophe. Since such a typical case of critical effect should be describable by a catastrophe, we may suspect that this behaviour is incorrect.

The most interesting effects predicted here are the transitions which may be expected between the equilibrium states revealed for $\Delta\varepsilon < 0$. They can occur for weak and very weak surface anchoring. In twisted nematic cells reversible transitions may occur between the deformed zero-field state and the lower state (see figure (h)) or between the lower and upper states (see figures (i) and (j)). They should be accompanied with a remarkable change in the optical transmission of the layer between polarizers.

Another interesting possibility results from the configuration of states shown in figure 1(*g*). The twisted nematic and supertwisted nematic cells could be switched between the upper and lower states by use of a nematic material with frequency dependent dielectric anisotropy. The low frequency signal, for which $\Delta\epsilon > 0$, causes the transition to the homeotropic state, whereas the high frequency signal, for which $\Delta\epsilon < 0$, gives the reverse transition to the twisted state. Both states are separated by an energy barrier and are stable in the absence of the field. The supertwisted structure with high Φ possesses these features at somewhat stronger anchoring than the twisted nematic cell, and seems to be more convenient.

The solution for the planar cell can be transferred to the problem of stationary states in the homeotropic cell with weak anchoring. In this case, ψ measures the deviation from the initial perpendicular orientation. The roles of k_{11} and k_{33} are interchanged. The behaviour presented in figures (*a*) and (*b*) is expected.

Analogous results can be obtained for the smectic C layer with a bookshelf geometry. The infinitely strong anchoring case was analysed by catastrophe theory method in [13]. The elastic properties of the system are determined by the constant B_2 . Under weak anchoring circumstances, the azimuthal angle ϕ has the same dependence on u as shown in figures (*a*) and (*b*).

References

- [1] RAPINI, A., and PAPOULAR, M., 1969, *J. Phys. Colloq.*, **C-4**, 54.
- [2] NEHRING, J., KMETZ, A. R., and SCHEFFER, T. J., 1976, *J. appl. Phys.*, **47**, 850.
- [3] BARBERO, G., and STRIGAZZI, A., 1981, *Nuovo Cim. B*, **64**, 101.
- [4] YANG, K. H., 1983, *J. Phys., Paris*, **44**, 1051.
- [5] BECKER, M. E., NEHRING, J., and SCHEFFER, T. J., 1985, *J. appl. Phys.*, **57**, 4539.
- [6] HANDSCHY, M. A., and CLARK, N. A., 1983, *Phys. Rev. Lett.*, **51**, 471.
- [7] ONG, H. L., MEYER, R. B., and HURD, A. J., 1984, *J. appl. Phys.*, **55**, 2809.
- [8] WELFORD, K. R., and SAMBLES, J. R., 1987, *Appl. Phys. Lett.*, **50**, 871.
- [9] BARBERO, G., and MEUTI, M., 1989, *Nuovo Cim. D*, **11**, 367.
- [10] POSTON, T., and STEWART, I., 1978, *Catastrophe Theory and its Applications* (Pitman).
- [11] DERFEL, G., 1988, *Liq. Crystals*, **3**, 1411.
- [12] DERFEL, G., 1990, *Liq. Crystals*, **8**, 331.
- [13] DERFEL, G., 1989, *Liq. Crystals*, **6**, 293.